Cancer "-omics"

Molecular Cancer Research

CREBBP/EP300 Bromodomain Inhibition Affects the Proliferation of AR-Positive Breast Cancer Cell Lines

Veronica Garcia-Carpizo, Sergio Ruiz-Llorente, Jacinto Sarmentero, Ana González-Corpas, and Maria J. Barrero

Abstract

Inhibitors that prevent the binding of bromodomains to acetylated histones hold therapeutic potential. However, the effects of targeting most of the 60 different bromodomains found in the human proteome remain unexplored. Here, we investigate the molecular mechanisms responsible for the antiproliferative properties of CREBBP/EP300 bromodomain inhibition in ER-negative breast cancer cell lines. We show using genetic and chemical approaches that CREBBP/EP300 bromodomains are critical to support the proliferation of the triple-negative breast cancer cell line MDA-MB-453. Analysis of the transcriptional pathways affected by CREBBP/EP300 bromodomain inhibitors reveals that the expression of genes associated with super-enhancers is downregulated, which in turn are occupied by very high levels of androgen receptor (AR) in MDA-MB-453 cells. Treatment of MDA-MB-453 with CREBBP/EP300 bromodomain inhibitors downregulates the expression of an AR-dependent signature distinctive of breast cancer tumors that express AR and causes a decrease in H3K27ac levels at AR-binding sites. In accordance, in prostate cancer cell lines that express AR CREBBP/EP300 bromodomain inhibitors downregulate the expression of genes bound by AR and associated with super-enhancers. In summary, we report that triple-negative breast cancer cell lines that express AR are particularly sensitive to CREBBP/EP300 bromodomain inhibitors and consequently these inhibitors hold potential to treat this type of cancer.

Implications: AR-dependent cancer cell lines are sensitive to CREBBP/EP300 bromodomain inhibitors.

Introduction

Bromodomain-containing proteins can act as effectors of histone acetylation as they are able to recognize acetylated residues in histone tails (1). During the last decade, it has been shown that inhibitors that block the interaction of bromodomains with acetylated residues have therapeutic potential (2). For example, inhibitors of the bromo and extraterminal domain (BET) family of bromodomain-containing proteins have been described to mediate important antiproliferative effects in cancer cell lines and are currently being tested in clinical trials (3). The mechanism of action of BET inhibitors consist on blocking the expression of oncogenes that are associated with enhancers with very high levels of histone acetylation known as super-enhancers (SE) and, in this way, inhibit oncogene-driven proliferation of cancer cells (4).

CREBBP and EP300 are closely related and likely redundant histone acetyltransferases (HAT) that share several conserved domains, including a HAT domain and a bromodomain. CREBBP/EP300 function primarily as coactivators for several transcription factors. The relevance of CREBBP/EP300 as targets for cancer treatment was first shown using inhibitors of the HAT activity (5–7). However, these early compounds, although promising, lacked potency or specificity (6, 8). Prompted by the preclinical success of BET bromodomains inhibitors, dual inhibitors of the bromodomains of CREBBP and EP300 have been recently developed (9–15). These inhibitors mediate several biological responses including antiproliferative effects in hematologic cancer cell lines, such as leukemia (11, 13, 16) and multiple myeloma (17) cell lines, and AR-positive prostate cancer cell lines (15). Moreover, EP300/CREBBP bromodomain inhibitors interfere with important oncogenic transcription programs driven by transcription factors such as MYC, IRF4, GATA1, and AR (13, 15–17).

In this study, we analyze the antiproliferative effects of CREBBP/EP300 bromodomain inhibitors in ER-negative breast cancer cell lines and the molecular mechanisms involved in such effects. Our results show that breast cancer cell lines that express high levels of AR are sensitive to EP300/CREBBP bromodomain inhibitors. Therefore, sensitivity to these inhibitors is not restricted to AR-positive prostate cancer but can be extended to other cancers in which AR plays a critical role in proliferation.

Materials and Methods

Cell lines and reagents

Human cancer cell lines MDA-MB-231, MDA-MB-453, SKBR3, DU145, PC3, LNCaP, VCaP, and 22RV1 were purchased from ATCC. CAL148 and MFM223 were purchased from DSMZ. SUM185PE was purchased from Asterand Bioscience. The identity

CNIO-Lilly Epigenetics Laboratory, Spanish National Cancer Research Center (CNIO), Madrid, Spain.

Note: Supplementary data for this article are available at Molecular Cancer Research Online (http://mcr.aacrjournals.org/).

Corresponding Author: Maria J. Barrero, Spanish National Cancer Research Center (CNIO), Melchor Fernandez Almagro 3, Madrid E-28029, Spain. Phone: 349-1732-8000; Fax: 349-1224-6980; E-mail: mjbarrero@cnio.es

doi: 10.1158/1541-7786.MCR-18-0719

of the cell lines was verified with short tandem repeat analysis. qPCR-based *Mycoplasma* test was routinely carried out once a month. Antibodies for Western blot analysis were obtained from the following sources: MYC (N-262) sc-764 from Santa Cruz Biotechnology, AR antibody 5153 from Cell Signaling Technology, H3K27ac ab4729 from Abcam, and ACTB (Ac-15) A5441 from Sigma-Aldrich.

Proliferation assays

To determine IC_{50}s, cells were grown in 96-well plates in the presence of increasing amounts of compound. Viability was determined at day seven using the CellTiter-Glow Luminescent Assay. IC_{50} values were calculated with the GraphPad Prims software using four-parameter variable-slope dose–response curve. For proliferation curves, MDA-MB-453 cells were cultured in DMEM with 10% charcoal-stripped FBS for one day. Then cells were trypsinized, counted, and plated (day 0) in triplicate for each condition, treated with vehicle, 2 μmol/L CBP30, 10 nmol/L DHT, or both and harvested and counted at the indicated days.

CRISPR-Cas9 gene editing and growth competition assays

We used the web tool cripsr.mit.edu to design the gRNAs (Supplementary Table S1). Only gRNAs with a quality score threshold above 80 were selected to minimize off-target effects. Nontarget gRNAs sequences were also included (18). gRNAs were cloned into the lentiviral vector pKLV-U6gRNA(BbsI)-PGKpuro2ABFP (Addgene plasmid # 50946) and lentiviral particles were generated as described previously (19). MDA-MB-453 cells previously modified to express Cas9 using pLentiCas9 Blast (Addgene plasmid # 52962; ref. 20) were infected. Four days after infection, we carried out growth competition assays by mixing an equal number of BFP^+/gRNA–expressing cells and non-gRNA–transduced parental Cas9-expressing cells (BFP^-). We determined the percentage of BFP^+ cells by flow cytometry at different days starting the day of the mixing (day 0) and calculated the fold depletion of the percentage of BFP^+ cells compared with day 0 (d0 $\%BFP^+$/dN $\%BFP^+$). At day 4 after infection, we confirmed the introduction of mutations by Sanger sequencing and that gRNAs targeting EP300 did not introduce mutations in CREBBP and vice versa. For the statistical analysis, for each gRNA, we calculated the percentage of growth inhibition at day 12 compared with day 0 and adjusted this percentage to the percentage of growth inhibition of the nontarget gRNAs. The adjusted percentages of growth inhibition for each gRNA obtained in three independent experiments were pooled into the following categories: nontarget, 5′ coding region, nonconserved amino acids, and conserved amino acids of the bromodomain. The differences between categories were analyzed using the Tukey–Kramer test (21).

RNA-seq

Cells were treated for 48 hours, trypsinized, and total RNA was extracted using the RNeasy Kit (Qiagen) including two biological replicates per condition. Library construction and sequencing were done as described previously (22). Alignment to human genome hg19 transcript assembly and differential expression was carried out using Nextpresso (23). Genes were considered as differentially expressed if FDR < 0.05.

Sequencing data has been deposited in the GEO repository with accession number GSE114937.

Gene set enrichment analysis

For GSEAPreranked (24), genes were preranked according to the statistic test of fold change for each treatment obtained in the RNA-seq analysis, setting "gene set" as the permutation method and with 1,000 permutations. ssGSEA was carried out using GenePattern (25). Genes sets used in this study can be found at the Molecular Signatures Database (http://software.broadinstitute.org/gsea/msigdb/index.jsp). MYC signature corresponds to MYC_UP.V1, KRAS signature corresponds to KRAS.LUNG.BREAST_UP.V1, the Doane and colleagues' apocrine signature corresponds to DOANE_BREAST_CANCER_CLASSES, and the Farmer and colleagues' apocrine signature corresponds to FARMER_BREAST_CANCER_APOCRINE_VS_BASAL.

ChIP-seq analysis

Sequencing analysis was carried out using Galaxy (https://toolshed.g2.bx.psu.edu/) and Galaxy Cistrome (http://cistrome.org/). Reads were mapped to the human genome build hg19 using Bowtie (26). Bigwig files were generated and displayed in the UCSC Genome Browser (http://genome.ucsc.edu/; ref. 27). Genomic intervals marked by H3K27ac were determined using MACS (28) and super-enhancers were identified using ROSE (4, 29). Briefly, H3K27ac intervals within 12.5 kb were stitched together and ranked by their H3K27ac signal. Super-enhancers were mapped to the nearest gene using GREAT (30). We identified super-enhancers acquired in breast cancer cells relative to normal mammary epithelial cells (HMEC) as described previously (22). Briefly, super-enhancers intervals in breast cancer cell lines and HMEC were concatenated and merged and the density of H3K27ac at these combined intervals in each sample was calculated. Regions with a ratio of H3K27ac signal in each cancer cell line versus HMEC higher than 10 fold were considered cancer-acquired super-enhancers (CASE) while regions with a ratio between 2 and 0.5 were considered shared super-enhancers (Normal SE). AR and FOXA1 abundance at super-enhancers and regular enhancers were calculated using bamToGFF (https://github.com/bradnerComputation/pipeline/blob/master/bamToGFF.py).

Chromatin immunoprecipitation

Chromatin immunoprecipitation (ChIP) assays were performed according to the Millipore protocol. MDA-MB-453 cells were treated with 5 μmol/L of CREBBP/EP300 bromodomain inhibitors for 1 hour and fixed with 1% formaldehyde for 20 minutes. Cross-linking was stopped with 0.125 mol/L glycine for 10 minutes, and chromatin was sheared and immunoprecipitated as described previously (22). Immunoprecipitated chromatin was purified and used for qPCR amplification using the oligonucleotides shown in Supplementary Table S1. qPCR signal was normalized to the input. To allow comparison between samples, signal was plotted relative to a negative control region located in gene HMGA2 (devoid of H3K27ac in this cell line).

Cell extracts

To interrogate the levels of AR and MYC by Western blot, soluble extracts were made by resuspending cell pellets in RIPA buffer (50 mmol/L Tris-Cl pH 7.4, 150 mmol/L NaCl, 1% NP40 and 0.25% Na-deoxycholate) supplemented with proteases inhibitors. After 30 minutes in ice, lysates were spun down and supernatants collected.

A

Cmpd	Protein	Domain	Breast cancer cell line IC_{50} (μmol/L)		
			MDA-MB-231	SKBR3	MDA-MB-453
JQ1	BRD4	BRD	0.004	0.007	0.017
C646	CREBBP/EP300	HAT	6.14	>20	3.49
CBP30	CREBBP/EP300	BRD	8.01	4.23	0.7
I-CBP112	CREBBP/EP300	BRD	>20	>20	2.6

B

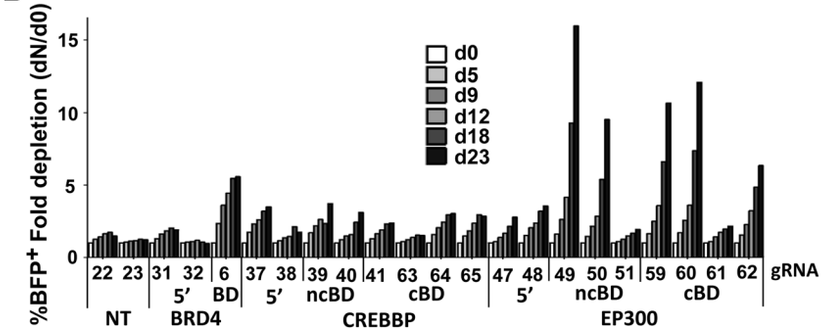

Figure 1.
MDA-MB-453 cells are proliferation sensitive to EP300/CREBBP inhibition. **A,** IC_{50} in μmol/L for the indicated compounds and ER^- breast cancer cell lines. **B,** Growth competition assays with MDA-MB-453 cells transduced with gRNAs targeting diverse domains of CREBBP, EP300, and BRD4 including 5′ coding region (5′), bromodomain (BD), nonconserved regions of bromodomain (ncBD), and conserved regions of bromodomain (cBD). Graph shows the fold depletion of BFP^+ cells (transduced with the indicated gRNAs) over BFP^- cells (nontransduced) at the indicated days compared with day 0. One representative experiment out of three independent experiments is shown. Statistical analysis of three independent experiments is shown in Supplementary Fig. S1.

Reporter assay

MDA-MB-453 cells were transfected with 1 μg of luciferase reporter vector containing a steroid receptor response element (Active Motif). The next day, cells were trypsinized and 30,000 cells per well plated on a 96-well plate in DMEM with 10% of charcoal-stripped FBS in the presence of 1 nmol/L dihydrotestosterone (DHT) and increasing concentrations of compound. Twenty-four hours later, cells were harvested, and luciferase activity measured using the LightSwitch Luciferase Assay Kit from Active Motif. Graphs and IC_{50} values were calculated with a four-parameter variable-slope dose–response curve using the GraphPad Prism software.

Cell-cycle analysis

Cells were fixed at 4°C with 70% ethanol for 1 hour and stained with propidium iodide (100 μg/mL), RNase A, and 0.1% Triton X-100 for 30 minutes. A BD LSRFortessa flow cytometer (BD Biosciences) was used to determine the cell-cycle distribution. Data were analyzed using the FlowJo software.

qPCR

RNA was obtained as described above, cDNA synthesized using the SuperScript First-Strand Synthesis System (Thermo Fisher Scientific), and real-time qPCR performed using the primers described in Supplementary Table S1.

Source of public data

Data on AR gene expression in cancer cell lines was downloaded from The Cancer Cell Line Encyclopedia (CCLE) website (http://www.broadinstitute.org/ccle/home). Data on AR, CREBBP, and EP300 gene expression in TCGA breast and prostate samples were downloaded from the UCSC Cancer Browser Xena. Data on EP300 and CREBBP mutation rate in different TCGA cancer subtypes was downloaded from GDC Data Portal. Correlation between AR and EP300 or CREBBP gene expression in TCGA prostate cancer tumors was interrogated at the cBioPortal. Source of raw data for ChIP-seq analysis was obtained through ArrayExpress accessions E-MTAB-1694 and E-MTAB-986 or GEO database accessions GSE29611, GSE49651, GSE51621, and GSE83860.

Results

MDA-MB-453 cells are proliferation-sensitive to CREBBP/EP300 inhibition

To gain insights into the potential therapeutic activity of CREBBP/EP300 inhibitors in breast cancer, we tested the sensitivity of three ER-negative breast cancer cell lines to CREBBP/EP300 inhibitors in proliferation assays. Of the three lines tested, MDA-MB-231 and MDA-MB-453 are triple-negative breast cancer cell lines while SKBR3 has *ERBB2* amplifications. Fig. 1A shows that while all cell lines are sensitive to the BET inhibitor JQ1, MDA-MB-453 is particularly sensitive to CREBBP/EP300 inhibitors. Despite the fact that CBP30 and I-CBP112 have been described to have good selectivity over other bromodomains (11, 31) we found pertinent to confirm the involvement of EP300 and CREBBP bromodomains in the proliferation of MDA-MB-453 cells using a recently described CRISPR-Cas9 genome editing approach to evaluate the relevance of protein domains in proliferation (32, 33). This method is based on the fact that one-third of randomly introduced mutations are in frame and are likely to generate a full-length protein with mutations in the particular domain targeted by the gRNA. More pronounced antiproliferative effects will be observed when targeting a domain relevant for proliferation than an irrelevant domain. We interrogated the effect of introducing mutations in the EP300 and CREBBP 5′ coding region and bromodomains in growth competition assays (Fig. 1B). We observed that introducing mutations in EP300 and CREBBP bromodomains caused antiproliferative effects when compared with mutations introduced in the 5′ coding region (Fig. 1B). Effects were more conspicuous when targeting conserved regions of the bromodomains and more significant for EP300 that CREBBP (Supplementary Fig. S1). Therefore, our CRISPR-Cas9 approach confirms that the bromodomains of CREBBP and EP300 are relevant to sustain the proliferation of MDA-MB-453.

CBP30 affects the expression of different subsets of genes in different cell lines

To understand the basis of the sensitivity of MDA-MB-453 cells to CREBBP/EP300 bromodomain inhibitors, we compared the transcriptional responses of MDA-MB-231, SKBR3, and

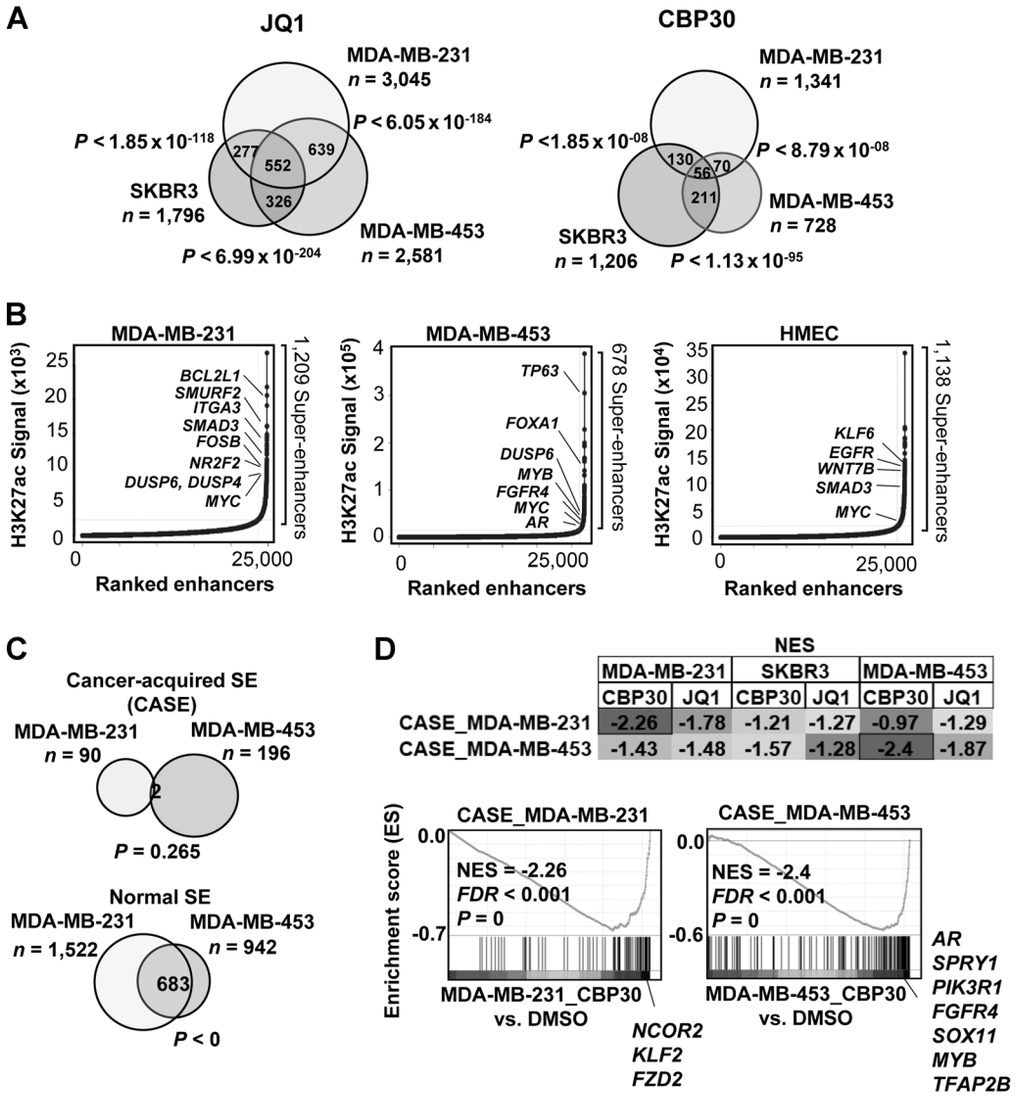

Figure 2.

CBP30 downregulates the expression of genes associated with CASEs in MDA-MB-453 and MDA-MB-231 cells. **A,** Overlap of genes downregulated by JQ1 or CBP30 in the different cell lines at FDR < 0.05. *P* values for the overlaps according to hypergeometric test are indicated. **B,** Graphs show enhancers ranked according to H3K27ac ChIP-signal (normalized sequencing reads) in the indicated cell lines. SEs were determined using ROSE according to H3K27ac levels. **C,** Overlap of genes associated with CASEs and genes associated with SEs in normal mammary epithelial cells (HMEC; normal SE). **D,** Gene set enrichment analysis (GSEA) normalized enrichment scores (NES) and enrichment plots for CASEs-associated genes in MDA-MB-231 and MDA-MB-453. Important genes in the leading edge associated with CASEs and downregulated by CBP30 are indicated.

MDA-MB-453 to these inhibitors and JQ1. Transcriptional responses to JQ1 had more amplitude than those to CBP30 in all lines (Supplementary Fig. S2A), which correlates with the higher sensitivity of all lines to this compound. CBP30 caused both upregulation and downregulation of genes in all three cell lines independently of their sensitivity to this compound (Supplementary Fig. S2A and S2B). We also found significant overlaps in genes affected by JQ1 and CBP30 in each cell line (Supplementary Fig. S2B). This finding is expected as both compounds target proteins related to acetylation. Because the amplitude of transcriptional effects did not correlate with the sensitivity of cell lines to CBP30, we suspected that the key to sensitivity could be related with the specific transcriptional programs differentially modulated between cell lines. Comparison of commonly downregulated genes in the three cell lines by JQ1 or CBP30 showed that overlap between cell lines of genes downregulated by CBP30 was much lower than of JQ1 (Fig. 2A) suggesting that the effects of CBP30 were more cell specific than those of JQ1. Moreover, gene set enrichment analysis (GSEA) showed that CBP30 affected the expression of genes related to different Reactome pathways depending on the cell line (Supplementary Fig. S3A). In MDA-MB-453, CBP30 upregulated genes involved in interferon signaling and downregulated genes involved in the activation of the prereplicative complex

(Supplementary Fig. S3B). Importantly, downregulation of the expression of genes involved in the prereplicative complex is likely to have important consequences for proliferation and this pathway is not downregulated by CBP30 in MDA-MB-231 and SKBR3.

CBP30 downregulates the expression of genes containing super-enhancers

Because EP300 and CREBBP mediate histone acetylation, we investigated the correlation of the genome-wide distribution of H3K27ac with the changes in gene expression caused by the CBP30 treatment. We used the software ROSE (4, 29) to identify SEs (Fig. 2B), in MDA-MB-231, MDA-MB-453, and in normal human mammary epithelial cells (HMCE). Next, we identified SEs that are present in cancer cell lines but not in HMECs and called them cancer-acquired super-enhancers (CASE). These SEs were probably acquired during the process of oncogenic transformation and are likely to control the expression of important genes involved in this process (22). Figure 2C shows that MDA-MB-231 and MDA-MB-453 do not share many genes associated with CASEs suggesting that the process of transformation of both cell lines entails different mechanisms. However, these cell lines share a large number of genes that are also associated with SEs in HMECs (Normal SEs), which probably reflects the common mammary origin of both cell lines. We next investigated the effects of CBP30 and JQ1 treatment in the expression of genes associated with CASEs in MDA-MB-453 or MDA-MB-231 using GSEA. Most significant enrichment was found CBP30 downregulated genes associated with CASEs in MDA-MB-453 (Fig. 2D). Is worth mentioning that CBP30 specifically affected the expression of genes associated with CASEs in a cell line–dependent manner.

CBP30 causes downregulation of the apocrine gene expression signature in MDA-MB-453 cells

We noticed that in MDA-MB-453 the expression of the CASE-associated gene *AR* is downregulated by the CBP30 treatment (Fig. 2D). Surprisingly, AR is very highly expressed in MDA-MB-453 compared with the expression levels in other CCLE cell lines (Fig. 3A). Analysis of motif enrichment (Fig. 3B) showed that AR-binding sites also contain motifs for FOXA1 and other members of the fork head family of transcription factors. FOXA1 is an important pioneer transcription factor that is relevant for AR function (34) and mediates accessibility to chromatin (35). Accordingly, analysis of binding profiles shows that FOXA1 is abundant at AR-binding sites in MDA-MB-453 (Fig. 3C). In addition, AR and FOXA1 are very abundant at SEs (Fig. 3D) and might play important roles in the maintenance of these elements.

AR expression is a hallmark of certain triple-negative breast cancers, described a decade ago and called apocrine or luminal androgen receptor (LAR; refs. 36, 37). MDA-MB-453 is a cell line representative of this type of breast cancer (38). Using single sample gene set enrichment analysis (ssGSEA) we compared the enrichment of transcriptional programs in particular signatures for each cell line and treatment, including a transcriptional signature from apocrine tumors (37). Because MDA-MB-231 has activating mutations in *KRAS* and SKBR3 has *MYC* amplifications, MYC and KRAS transcriptional signatures were also tested. As expected, the KRAS transcriptional signature is enriched in MDA-MB-321 compared with the other cell lines and is significantly downregulated by the treatments (Fig. 3E). MYC transcriptional signature is enriched in both SKBR3 and MDA-MB-453 and also downregulated by treatments. The apocrine signature is particularly enriched in MDA-MB-453 and downregulated with treatments. Importantly, enrichment in this signature correlates with the sensitivity of the cell lines to CBP30. Therefore, we conclude that CBP30 differentially downregulates the expression of genes that are distinctive of triple-negative breast cancers apocrine subtype in MDA-MB-453 cells.

CREBBP/EP300 bromodomain inhibitors revert the effects of the AR agonist 5α-dihydrotestosterone

AR agonists such as 5α-dihydrotestosterone (DHT) have been described to stimulate the growth of MDA-MB-453 cells and this effect can be reverted by AR antagonists (39). To confirm the involvement of CBP30 in inhibiting AR function, we carried out similar experiments. Figure 3F shows that at 10 nmol/L DHT has marginal effects on MDA-MB-453 cells growth; however, it can counteract the antiproliferative effects caused by CBP30 indicating that DHT and CBP30 have antagonistic effects on MDA-MB-453 growth, likely by affecting the same pathway.

To confirm this idea, we tested the ability of CBP30 and two additional CREBBP/EP300 bromodomain inhibitors CPI644 (14) and GNE-272 (13) to interfere with AR-driven transcription in a luciferase reporter assay. MDA-MB-453 were transfected with a luciferase reporter construct that responds to DHT and cultured in the presence of DHT and increasing concentrations of compounds, including the AR antagonist enzalutamide. Figure 3G shows that like enzalutamide, the three CREBBP/EP300 bromodomain inhibitors are able to block the induction of the reporter by DHT. These results suggest that CREBBP/EP300 bromodomain inhibitors interfere with the ability of AR to stimulate transcription.

CBP30 causes downregulation of MYC expression

Because we found downregulation of the MYC transcriptional signature in two of the tested cell lines (Fig. 3E), we investigated whether MYC was downregulated by the treatments. Supplementary Figure S4 shows that MYC expression is downregulated by CBP30 in SKBR3 and MDA-MB-453. Because SKBR3 is not particularly sensitive to CBP30, we conclude that MYC amplifications or downregulation of MYC expression and MYC-driven transcriptional programs is not enough to predict sensitivity to CREBBP/EP300 bromodomain inhibitors. Importantly, MYC has been described to be a target of AR in MDA-MB-453 that in turn contributes to stimulate AR-driven transcription of many AR target genes (40).

CREBBP/EP300 bromodomain inhibitors downregulate the levels of H3K27ac at AR target genes

Our next goal was to investigate further the mechanism of action of CREBBP/EP300 bromodomain inhibitors in MDA-MB-453. To select the most likely CREBBP/EP300 direct target genes we identified genes in the GSEA leading edge (genes from the gene set that contribute the most to the enrichment score) of the apocrine signature described by Doane and colleagues (37), that are also in the leading edge of the apocrine signature described by Farmer and colleagues (36), are associated with SEs and have AR-binding sites (Supplementary Fig. S5A and S5B). As expected, most of these genes are highly expressed in MDA-MB-453 compared with the other cell lines (Supplementary Fig. S5C). Among these genes, we found the transcription factor *TFAP2B*, a member of the TFAP2 family for which binding motifs were found in AR-

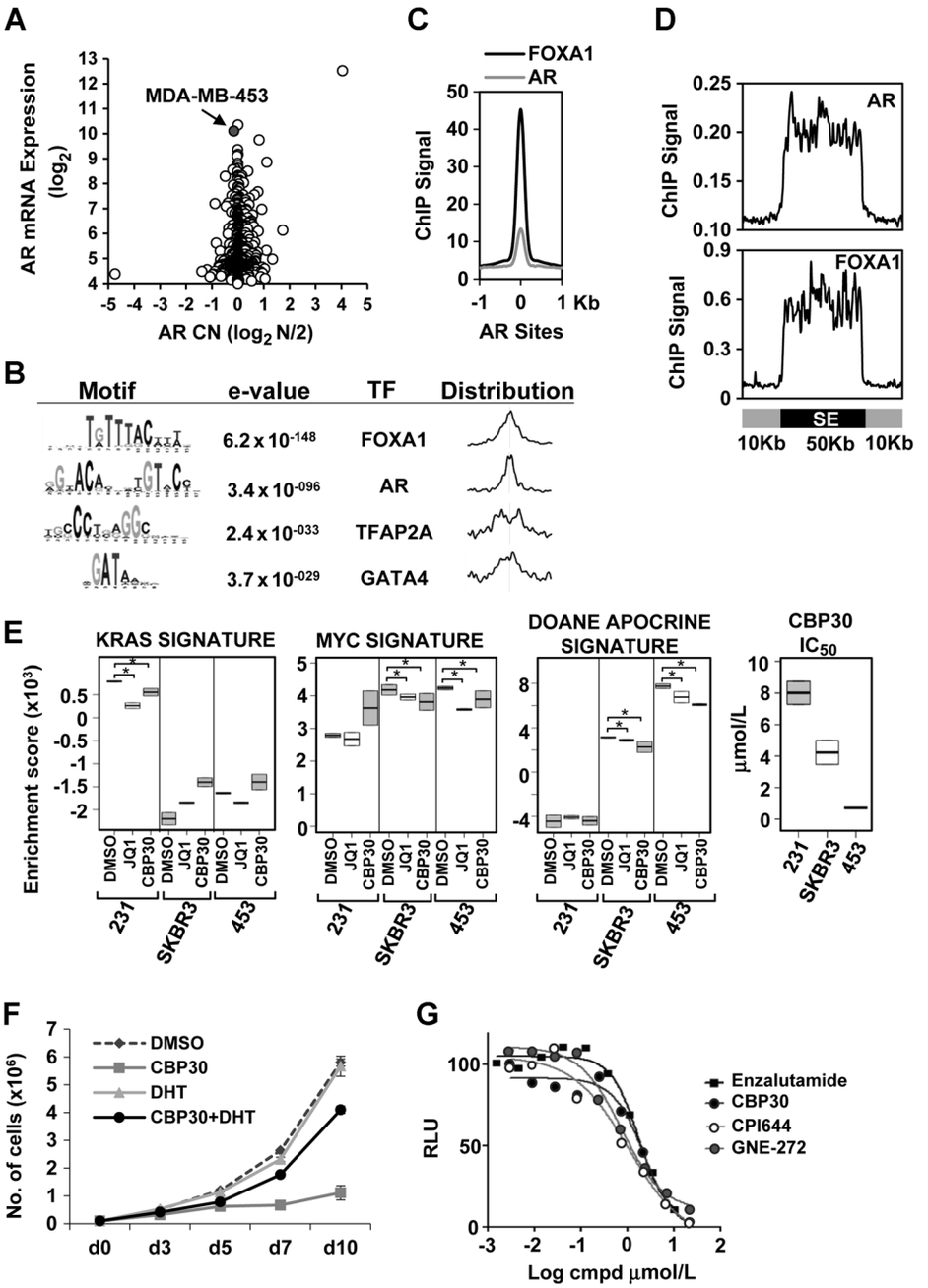

Figure 3.

AR is highly expressed in MDA-MB-453 and is very abundant at SEs. **A,** Levels of AR mRNA and copy number (CN) in CCLE lines. **B,** Analysis of motifs enrichment at AR-binding sites in MDA-MB-453 shows enrichment of fork head, GATA, and TFAP2 families of transcription factors. The most enriched representative of each family is shown. **C,** ChIP-signal (normalized sequencing reads) of FOXA1 and AR in AR-binding sites in MDA-MB-453. **D,** ChIP-signal (normalized sequencing reads) of AR and FOXA1 in SEs in MDA-MB-453 cells. **E,** Enrichment scores obtained using ssGSEA for MYC, KRAS, and APOCRINE signatures for each cell line and treatment. Right, IC_{50}s for CBP30 in each cell line. $^*P < 0.05$. **F,** Growth curve showing the number of MDA-MB-453 cells cultured in the presence of vehicle, 2 µmol/L CBP30, or/and 10 nmol/L DHT at different days. **G,** Luciferase reporter assay in MDA-MB-453 cells transfected with a reporter construct driving the expression of luciferase in response to DHT. Graph shows relative luciferase units (RLU) in the presence of 1 nmol/L DHT and increasing concentrations of the tested compounds. The mean of four independent experiments is shown. IC_{50}s for the different compounds were 1.71 µmol/L for enzalutamide, 2.27 µmol/L for CBP30, 1.04 µmol/L for CPI644, and 0.74 µmol/L for GNE-272.

binding sites in MDA-MB-453 (Fig. 3B). The dynamics of response of a subset of these genes to three different CREBBP/EP300 bromodomain inhibitors was evaluated by qPCR at different times after treatment (Fig. 4A). The three compounds displayed a very similar pattern of response in the selected genes, suggesting that the effects of the compounds are on target. Transcription factors MYC, AR, and TFAP2B showed the faster responses, which might contribute to the consequent downregulation of their target genes. *MYC* mRNA was already downregulated 30 minutes after the addition of the compounds followed by a decrease in protein levels at 2 hours of compound treatment (Fig. 4B). *AR* mRNA levels reached a minimum at 6 hours of treatment; however, no clear correlation with changes in protein levels was observed (Fig. 4B).

Our previous work has demonstrated that CREBBP/EP300 bromodomain inhibitors are able to displace CREBBP and EP300 from acetylated genomic regions resulting in lower levels of histone acetylation at these sites (16). Therefore, we asked whether CREBBP/EP300 bromodomain inhibitors could be reducing the levels of H3K27ac at AR-binding sites located in SEs (see Supplementary Fig. S5B for location of binding sites) and that likely play a role in the expression of genes shown in Fig. 4A. To rule out that the changes in H3K27ac could be due to a decrease in the expression of AR and consequent decrease in the occupancy of

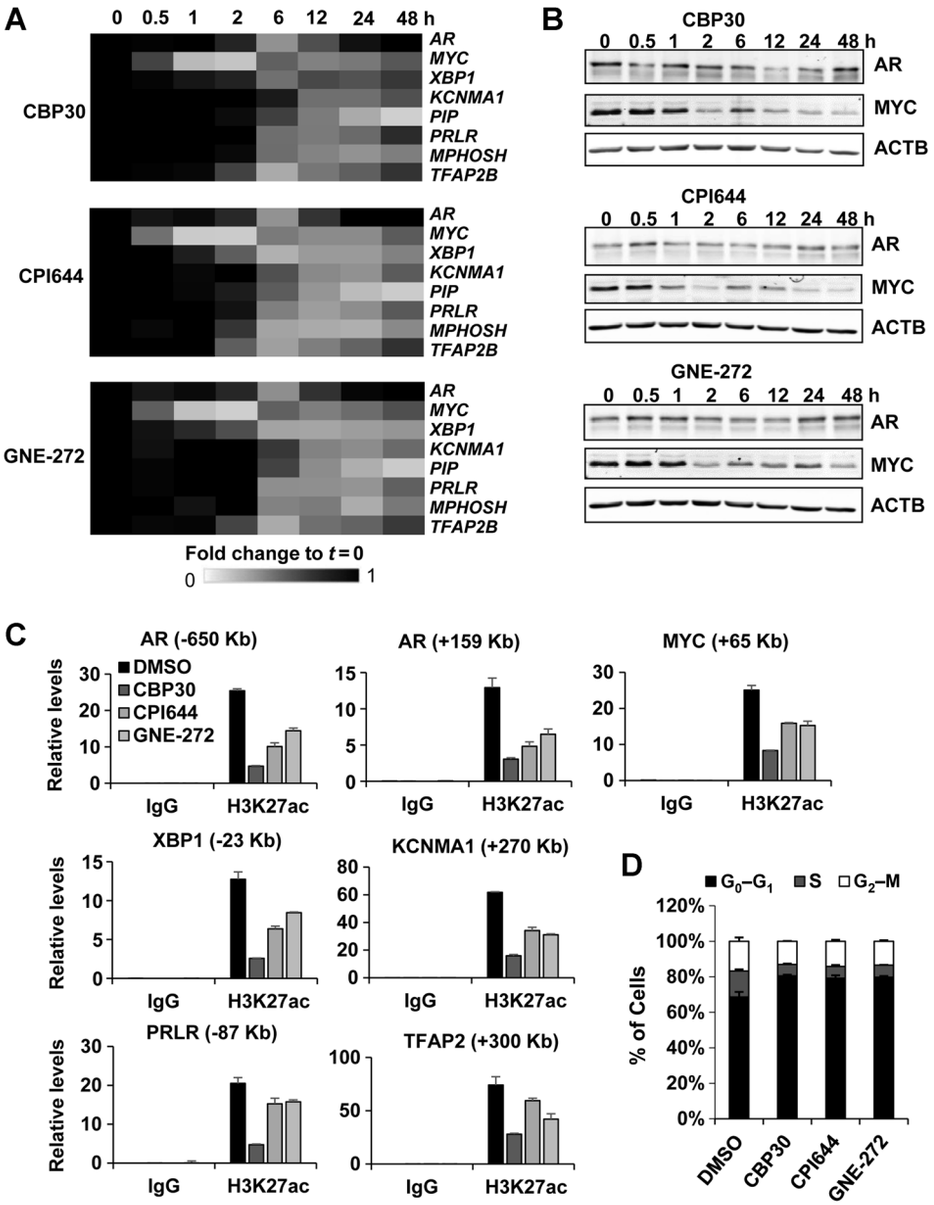

Figure 4.
Gene expression responses to different CREBBP/EP300 bromodomain inhibitors. **A,** Fold changes in gene expression relative to time 0 of selected genes along time (hours) caused by the treatment of MDA-MB-453 with 2 μmol/L of the indicated CREBBP/EP300 bromodomain inhibitors. **B,** Levels of AR and MYC proteins in the same experiment as **A**. **C,** ChIP-qPCR showing enrichment of H3K27ac in the indicated genes in MDA-MB-453 cells treated with vehicle (DMSO) and 5 μmol/L each CREBBP/EP300 bromodomain inhibitor for 1 hour. Levels were normalized to the input and plotted relative to a negative control region. IgGs were used as a negative control for the immunoprecipitation. The position of the amplicons relative to the transcription start site of each gene is indicated. Graph shows the mean and SD of three quantifications. **D,** Cell-cycle distribution analysis of MDA-MB-453 cells treated with vehicle (DMSO) and 2 μmol/L each CREBBP/EP300 bromodomain inhibitor for 72 hours. Graph shows the mean and SD of three replicates. All treatments caused significant changes in the percentage of cell in G_0–G_1 and S-phase compared with DMSO at a $P < 0.05$.

its binding sites, we conducted ChIP experiments after 1 hour of CREBBP/EP300 bromodomain inhibitors' treatment. At this time, levels of AR are not significantly affected by the treatments (Fig. 4A and B). Figure 4C shows that the treatment with CREBBP/EP300 bromodomain inhibitors causes a decrease in the H3K27ac levels at all genomic locations tested suggesting that CREBBP/EP300 bromodomain inhibitors interfere with the ability of CREBBP/EP300 to keep high levels of histone acetylation at AR-binding sites.

In agreement with the effects in proliferation, gene expression, and histone acetylation, CREBBP/EP300 bromodomain inhibitors caused significant changes in MDA-MB-453 cell-cycle distribution. An increase in the percentage of cells in G_0–G_1 and a decrease in the percentage of cells in S-phase was observed after 72 hours of compound treatment compared with vehicle (Fig. 4D). Treatments did not cause significant changes in the percentage of cells in G_2–M. Therefore, we conclude that the inhibitors are affecting the proliferation of MDA-MB-453 mainly through G_0–G_1 phase cell-cycle arrest.

CREBBP/EP300 bromodomain inhibitors affect the proliferation of apocrine breast cancer cell lines

Our data suggest that tumors with high expression of AR might be sensitive to CREBBP/EP300 bromodomain inhibitors. To find additional lines potentially sensitive to these inhibitors, we selected several triple-negative breast cancer cell lines classified as apocrine according to their transcriptional programs (38) and the levels of AR expression confirmed by Western blot analysis. Figure 5A shows that three of these lines, MDA-MB-453, SUM185PE, and MFM223, express substantial levels of AR,

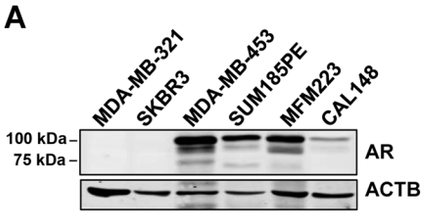

B

	IC_{50} (μmol/L)			
	MDA-MB-453	SUM185 PE	MFM223	CAL148
I-CBP112	2.6	>20	>20	>20
CBP30	0.7	3.35	5.57	>20
CPI644	0.64	4.3	4.59	>20
CPI637	0.51	2.33	2.62	>20
GNE-272	0.34	>20	7.78	>20

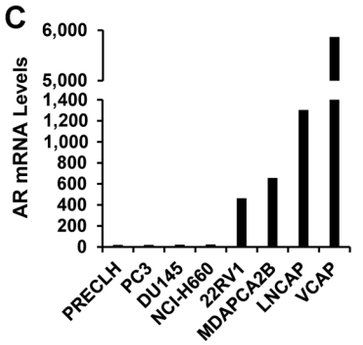

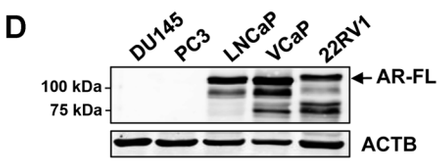

E

	AR Negative		AR Positive		
	DU145	PC3	LNCaP	VCaP	22Rv1
CBP30	>20	>20	1.28	1.74	0.6
CPI644	>20	>20	1.92	0.62	1.6
GNE-272	>20	>20	1.99	0.65	0.05

Figure 5.
Cell lines that express high levels of AR respond to CREBBP/EP300 inhibitors. **A,** Western blot analysis shows the expression of AR in ER^- breast cancer cell lines. **B,** IC_{50}s in μmol/L for different CREBBP/EP300 bromodomain inhibitors in AR-expressing breast cancer cell lines. **C,** Levels of *AR* mRNA expression in prostate cancer cell lines according to CCLE data. **D,** Expression of AR determined by Western blot analysis in prostate cancer cell lines. **E,** IC_{50}s in μmol/L for different CREBBP/EP300 bromodomain inhibitors in AR^- and AR^+ prostate cancer cell lines.

while CAL148 expresses very low levels despite being classified as an apocrine cell line. Sensitivity to CREBBP/EP300 inhibitors correlate with the levels of expression of AR in the tested cell lines, being CAL148 the less sensitive line (Fig. 5B).

CREBBP/EP300 bromodomain inhibitors affect the proliferation of AR-dependent prostate cancer cell lines

Finally, to confirm the correlation between sensitivity to CREBBP/EP300 bromodomain inhibitors and AR expression, we interrogated the sensitivity of several prostate cancer cell lines. Because expression of AR is a hallmark of a subset of prostate cancers, we selected several prostate cancer cell lines that according to mRNA levels express low or high levels of AR (Fig. 5C) and confirmed the expression of AR by Western blot analysis (Fig. 5D). Cell lines positive for AR expression are proliferation sensitive to CREBBP/EP300 inhibitors, including the androgen-resistant line 22Rv1, while AR^- lines are not (Fig. 5E). These results are in agreement with a recent report describing that AR^+ prostate cancer cell lines are sensitive to CREBBP/EP300 bromodomain inhibitors (15). We next identified SEs in the sensitive line LNCaP using the H3K27ac signal (Fig. 6A) and confirmed that AR is very abundant at SEs compared with regular enhancers in this cell line (Fig. 6B). Next, we selected genes that have SEs and are occupied by AR in LNCaP (Supplementary Fig. S6) and have been described to play critical roles in prostate cancer, and evaluated the transcriptional responses of these genes to three CREBBP/EP300 bromodomain inhibitors along time (Fig. 6C and D). Strikingly, the dynamics of response of AR and MYC to the CREBBP/EP300 inhibitors is very similar to the one found in MDA-MB-453, suggesting that similar mechanisms of response are involved in both cell lines.

No evidence of loss or gain of CREBBP/EP300 function in AR-dependent breast and prostate cancers

Inactivating mutations in CREBBP and EP300 have been described in some types of tumors suggesting that in certain cancers these genes could have tumor suppressor functions (41). Therefore, we investigated the rate of CREBBP/EP300 mutations in breast and prostate cancers. According to The Cancer Genome Atlas (TCGA), breast and prostate cancers have a low rate of mutations in these genes (Supplementary Fig. S7A). Next, we identified apocrine tumors in the TCGA breast tumors following a similar method to Doane and colleagues (37). We selected tumors classified as estrogen receptor–negative, progesterone receptor–negative (ER^-/PR^-) by the TCGA and calculated for each tumor the enrichment in the apocrine signature described by Doane and colleagues (37) using ssGSEA. Tumors with positive enrichment for this signature were considered apocrine. As expected, apocrine tumors express high levels of *AR* mRNA compared with ER^-/PR^- tumors that are not apocrine (Supplementary Fig. S7B). The rate of *CREBBP* or *EP300* genetic alterations in apocrine tumors was low, including one CREBBP mutation, one EP300 mutation, one CREBBP amplification, and one EP300 amplification in a total of 45 tumors.

Next, we investigated the expression of EP300 or CREBBP in normal tissues and different types of tumors. The expression of *EP300* and *CREBBP* in breast and prostate tumors and their corresponding normal tissues was high with a tendency to be downregulated in cancer samples (Supplementary Fig. S7C and S7D), including in apocrine breast cancer tumors. No significant differences in *EP300* or *CREBBP* expression where found between ER^-/PR^- apocrine and nonapocrine tumors. Despite this, a positive correlation between *EP300* or *CREBBP* and *AR* expression could be detected in breast (Supplementary Fig. S7E) and more dramatically in prostate cancer samples (Supplementary Fig. S7F) when all tumor types were considered. However, it is important to notice that all tumors express high levels of *CREBBP/EP300* compared with the variable levels of *AR* expression. These data suggest that in breast and prostate cancer, gain or loss of EP300 or CREBBP function is not common and sensitivity to CREBBP/EP300 inhibitors likely relays in the levels of AR expression rather than CREBBP/EP300 alterations.

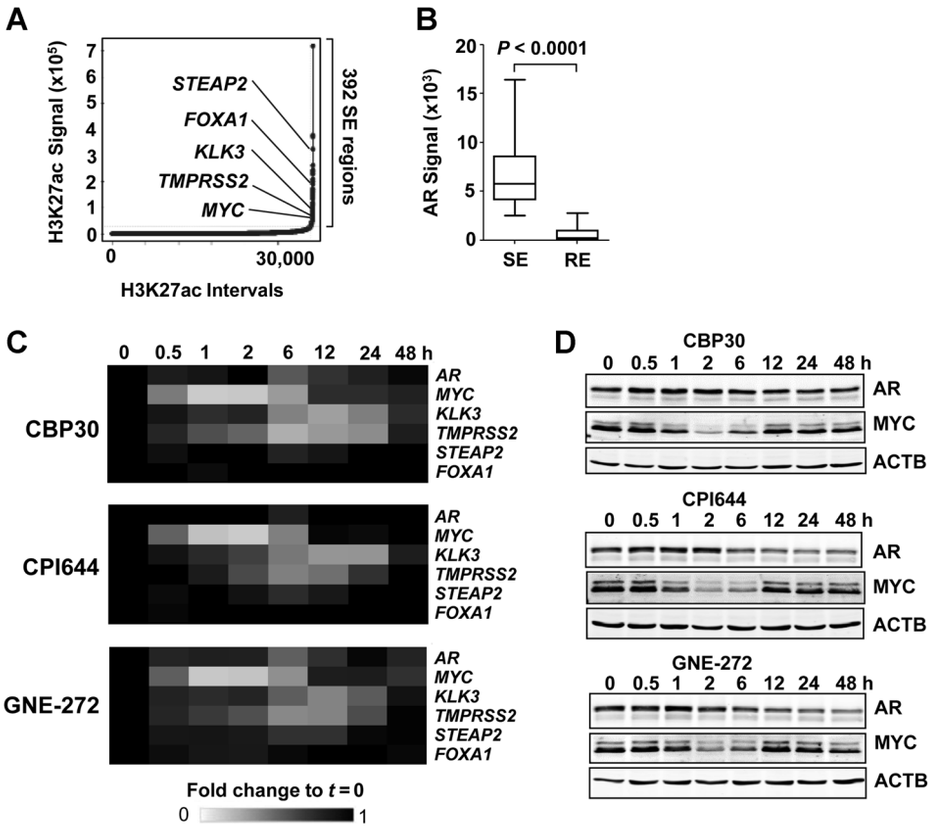

Figure 6.
Effects of different CREBBP/EP300 bromodomain inhibitors. **A,** Enhancers ranked according to H3K27ac ChIP signal (normalized sequencing reads) in LNCaP. **B,** AR ChIP signal (normalized sequencing reads) at SEs and regular enhancers (RE) in LNCaP. **C,** Fold changes in gene expression relative to time 0 of selected genes in LNCaP cells treated with 2 μmol/L of the indicated CREBBP/EP300 bromodomain inhibitors and at different times. **D,** Levels of AR and MYC proteins in the same experiment as in **C**.

Discussion

Our results show that CREBBP/EP300 bromodomain inhibitors have antiproliferative effects in a subset of cancer cell lines from solid tumors. In AR^+ tumors, such as apocrine/LAR breast cancer and prostate cancers, these inhibitors interfere with AR-driven transcription and impair the proliferation of cancer cells. CREBBP and/or EP300 have been described to interact with AR, acting as transcriptional coactivators and modulators of AR stability through its acetylation (42–44). In apocrine breast cancer cells, AR is likely to be an important transcription factor that mediates the recruitment of CREBBP/EP300 to SEs and contribute to maintain their high levels of acetylation.

During the last years, combinatorial therapies have emerged as an alternative to reduce toxicity and fight resistance. Although we have demonstrated therapeutic potential for CREBBP/EP300 bromodomain inhibitors as a single agent in preclinical models, combinations with other therapeutic agents might be of benefit. AR antagonists such as bicalutamide and enzalutamide have been suggested as a therapeutic option for ER^-/AR^+ breast cancers (39, 45). A typical mechanism of resistance to AR antagonists in prostate cancer is the expression of AR mRNA variants that lack the ligand-binding domain. Although not much is known about potential mechanisms of resistance to these drugs in breast cancer, cotreatment with CREBBP/EP300 bromodomain inhibitors might help to fight resistance to AR antagonists because most of the AR variants that lack the ligand-binding domain still retain the domain that interacts with CREBBP/EP300 (46–48). The fact that the androgen-resistant line 22Rv1 that expresses truncated forms of AR is sensitive to CREBPP/EP300 bromodomain inhibitors further reinforces this possibility. In addition, MDA-MB-453 has been often classified as a $Her2^+$ cell line despite absence of amplifications in the *ERBB2* locus. Upregulation of *ERBB2* expression has been described in ER^- breast cancer cell lines with apocrine phenotype (37, 39), which suggests that patients with ER^-/AR^+ breast cancers might benefit from combinations of drugs targeting Her2 and CREBBP/EP300.

Downregulation of MYC has been previously proposed to be a hallmark of CREBBP/EP300 bromodomain inhibitors action (13, 17). We observed that the CREBBP/EP300 bromodomain inhibitors cause downregulation of MYC and MYC-driven transcriptional programs in two of the cell lines tested. However, sensitivity does not correlate with high levels of MYC expression or downregulation of MYC expression. Although downregulation of MYC is not a predictor of sensitivity it is very likely that it contributes to the transcriptional effects that mediate sensitivity. For example, MYC is an important transcription factor that contributes to the regulation of AR target genes (40). Also, cooperation between IRF4 or GATA1 and MYC has been involved in the sensitivity to CREBBP/EP300 inhibitors in multiple myeloma and leukemia (16, 17). Therefore, we propose that MYC in cooperation with another critical transcription factor rather than MYC alone might hold the key to sensitivity.

CREBBP/EP300 bromodomain inhibitors are promising anticancer compounds that are currently being tested in preclinical models. CREBBP and EP300 are transcriptional coactivators that can interact with several transcription factors and therefore are susceptible to modulate a potential number of transcriptional programs. Accordingly, we expect that CREBBP/EP300

bromodomain inhibitors will be effective in treating cancers governed by other transcription factors that depend on CREBBP/EP300 to function. A better understanding of the dependencies of transcription factors on CREBBP/EP300 as well as the dependencies of certain cancers on the action of oncogenic transcription factors will be crucial to understand the vulnerabilities of different types of tumors to CREBBP/EP300 bromodomain inhibitors. Compared with BET inhibitors, for which many cancer vulnerabilities have been described in preclinical models, CREBBP/EP300 bromodomain inhibitors are likely to have a more restricted pattern of action. The main member of the BET family BRD4 plays essential roles in transcription through its interaction with P-TEFb and the potential toxicity of its inhibitors remains an issue that is currently being tested in clinical trials (3). It is worth noticing that the CREBBP/EP300 bromodomain inhibitor GNE-272 does not cause significant toxicity in xenograft mouse models (13). All these findings suggest a more cancer subtype–oriented treatment and perhaps lower toxicity for CREBBP/EP300 bromodomain inhibitors compared with BRD4 inhibitors.

Our results are in line with recent reports showing that AR^+ prostate cancer cell lines are sensitive to CREBBP/EP300 bromodomain and catalytic inhibitors (13, 49). Importantly, we show that sensitivity of AR^+ cancers can be extended to breast cancer cell lines that express AR. Therefore, expression levels of AR might be used to select patients likely to respond to CREBBP/EP300 bromodomain inhibitors in a variety of cancers.

Disclosure of Potential Conflicts of Interest

M.J. Barrero reports receiving other commercial research support from Eli Lilly. No potential conflicts of interest were disclosed by the other authors.

Authors' Contributions

Conception and design: M.J. Barrero
Development of methodology: M.J. Barrero
Acquisition of data (provided animals, acquired and managed patients, provided facilities, etc.): V. Garcia-Carpizo, S. Ruiz-Llorente, A. González-Corpas
Analysis and interpretation of data (e.g., statistical analysis, biostatistics, computational analysis): V. Garcia-Carpizo, M.J. Barrero
Writing, review, and/or revision of the manuscript: V. Garcia-Carpizo, M.J. Barrero
Administrative, technical, or material support (i.e., reporting or organizing data, constructing databases): V. Garcia-Carpizo, J. Sarmentero
Study supervision: M.J. Barrero

Acknowledgments

The authors would like to thank the Spanish State Public Employment Service (SEPE) for support during the preparation of this manuscript. We thank the Flow Cytometry and Genomics Units, O. Graña and the Bioinformatics Unit at the CNIO for assistance in the bioinformatics analysis, and M. Serrano and M. Malumbres for constructive discussions. This work was funded by Eli Lilly and Company

The costs of publication of this article were defrayed in part by the payment of page charges. This article must therefore be hereby marked *advertisement* in accordance with 18 U.S.C. Section 1734 solely to indicate this fact.

Received July 6, 2018; revised October 10, 2018; accepted December 14, 2018; published first January 3, 2019.

References

1. Dhalluin C, Carlson JE, Zeng L, He C, Aggarwal AK, Zhou MM. Structure and ligand of a histone acetyltransferase bromodomain. Nature 1999; 399:491–6.
2. Muller S, Filippakopoulos P, Knapp S. Bromodomains as therapeutic targets. Expert Rev Mol Med 2011;13:e29.
3. Andrieu G, Belkina AC, Denis GV. Clinical trials for BET inhibitors run ahead of the science. Drug Discov Today Technol 2016;19:45–50.
4. Lovén J, Hoke HA, Lin CY, Lau A, Orlando DA, Vakoc CR, et al. Selective inhibition of tumor oncogenes by disruption of super-enhancers. Cell 2013;153:320–34.
5. Santer FR, Höschele PP, Oh SJ, Erb HH, Bouchal J, Cavarretta IT, et al. Inhibition of the acetyltransferases p300 and CBP reveals a targetable function for p300 in the survival and invasion pathways of prostate cancer cell lines. Mol Cancer Ther 2011;10:1644–55.
6. Yang H, Pinello CE, Luo J, Li D, Wang Y, Zhao LY, et al. Small-Molecule Inhibitors of Acetyltransferase p300 identified by high-throughput screening are potent anticancer agents. Mol Cancer Ther 2013;12:610–20.
7. Bowers EM, Yan G, Mukherjee C, Orry A, Wang L, Holbert MA, et al. Virtual Ligand Screening of the p300/CBP histone acetyltransferase: identification of a selective small molecule inhibitor. Chem Biol 2010;17:471–82.
8. Shrimp JH, Sorum AW, Garlick JM, Guasch L, Nicklaus MC, Meier JL. Characterizing the covalent targets of a small molecule inhibitor of the lysine acetyltransferase P300. ACS Med Chem Lett 2016;7:151–5.
9. Hay DA, Fedorov O, Martin S, Singleton DC, Tallant C, Wells C, et al. Discovery and optimization of small-molecule ligands for the CBP/p300 bromodomains. J Am Chem Soc 2014;136:9308–19.
10. Chekler EL, Pellegrino JA, Lanz TA, Denny RA, Flick AC, Coe J, et al. Transcriptional profiling of a selective CREB binding protein bromodomain inhibitor highlights therapeutic opportunities. Chem Biol 2015; 22:1588–96.
11. Picaud S, Fedorov O, Thanasopoulou A, Leonards K, Jones K, Meier J, et al. Generation of a selective small molecule inhibitor of the CBP/p300 bromodomain for leukemia therapy. Cancer Res 2015;75:5106–19.
12. Xu M, Unzue A, Dong J, Spiliotopoulos D, Nevado C, Caflisch A. Discovery of CREBBP bromodomain inhibitors by high-throughput docking and hit optimization guided by molecular dynamics. J Med Chem 2016;59:1340–9.
13. Crawford TD, Romero FA, Lai KW, Tsui V, Taylor AM, de Leon Boenig G, et al. Discovery of a potent and selective in vivo probe (GNE-272) for the bromodomains of CBP/EP300. J Med Chem 2016;59:10549–63.
14. Ghosh S, Taylor A, Chin M, Huang HR, Conery AR, Mertz JA, et al. Regulatory T cell modulation by CBP/EP300 bromodomain inhibition. J Biol Chem 2016;291:13014–27.
15. Jin L, Garcia J, Chan E, de la Cruz C, Segal E, Merchant M, et al. Therapeutic Targeting of the CBP/p300 bromodomain blocks the growth of castration-resistant prostate cancer. Cancer Res 2017;77:5564–75.
16. Garcia-Carpizo V, Ruiz-Llorente S, Sarmentero J, Graña-Castro O, Pisano DG, Barrero MJ. CREBBP/EP300 bromodomains are critical to sustain the GATA1/MYC regulatory axis in proliferation. Epigenetics Chromatin 2018;11:30.
17. Conery AR, Centore RC, Neiss A, Keller PJ, Joshi S, Spillane KL, et al. Bromodomain inhibition of the transcriptional coactivators CBP/EP300 as a therapeutic strategy to target the IRF4 network in multiple myeloma. Elife 2016;5:e10483.
18. Wang T, Wei JJ, Sabatini DM, Lander ES. Genetic screens in human cells using the CRISPR-Cas9 System. Science 2014;343:80–4.
19. Wiznerowicz M, Trono D. Conditional suppression of cellular genes: lentivirus vector-mediated drug-inducible RNA interference. J Virol 2003; 77:8957–61.
20. Sanjana NE, Shalem O, Zhang F. Improved vectors and genome-wide libraries for CRISPR screening. Nat Methods 2014;11:783–4.
21. Tukey JW. Comparing individual means in the analysis of variance. Biometrics 1949;5:99–114.
22. García-Carpizo V, Sarmentero J, Han B, Graña O, Ruiz-Llorente S, Pisano DG, et al. NSD2 contributes to oncogenic RAS-driven transcription in lung

cancer cells through long-range epigenetic activation. Sci Rep 2016; 6:32952.
23. Graña O, Rubio-Camarillo M, Fdez-Riverola F, Pisano DG, Glez-Peña D. Nextpresso: next generation sequencing expression analysis pipeline. Curr Bioinform 2018;13:583–91.
24. Subramanian A, Tamayo P, Mootha VK, Mukherjee S, Ebert BL. Gene set enrichment analysis : a knowledge-based approach for interpreting genome-wide. Proc Natl Acad Sci U S A 2005;102:15545–50.
25. Reich M, Liefeld T, Gould J, Lerner J, Tamayo P, Mesirov JP. GenePattern 2.0 [2]. Nat Genet 2006;38:500–1.
26. Langmead B, Trapnell C, Pop M, Salzberg SL. Ultrafast and memory-efficient alignment of short DNA sequences to the human genome. Genome Biol 2009;10:R25.
27. Kent WJ, Sugnet CW, Furey TS, Roskin KM, Pringle TH, Zahler AM, et al. The human genome browser at UCSC. Genome Res 2002;12:996–1006.
28. Zhang Y, Liu T, Meyer CA, Eeckhoute J, Johnson DS, Bernstein BE, et al. Model-based analysis of ChIP-Seq (MACS). Genome Biol 2008;9: R137.
29. Whyte WA, Orlando DA, Hnisz D, Abraham BJ, Lin CY, Kagey MH, et al. Master transcription factors and mediator establish super-enhancers at key cell identity genes. Cell 2013;153:307–19.
30. McLean CY, Bristor D, Hiller M, Clarke SL, Schaar BT, Lowe CB, et al. GREAT improves functional interpretation of cis-regulatory regions. Nat Biotechnol 2010;28:495–501.
31. Hammitzsch A, Tallant C, Fedorov O, O'Mahony A, Brennan PE, Hay DA, et al. CBP30, a selective CBP/p300 bromodomain inhibitor, suppresses human Th17 responses. Proc Natl Acad Sci U S A 2015;112: 10768–73.
32. Shi J, Wang E, Milazzo JP, Wang Z, Kinney JB, Vakoc CR. Discovery of cancer drug targets by CRISPR-Cas9 screening of protein domains. Nat Biotechnol 2015;33:661–7.
33. Munoz DM, Cassiani PJ, Li L, Billy E, Korn JM, Jones MD, et al. CRISPR screens provide a comprehensive assessment of cancer vulnerabilities but generate false-positive hits for highly amplified genomic regions. Cancer Discov 2016;6:900–13.
34. Robinson JL, MacArthur S, Ross-Innes CS, Tilley WD, Neal DE, Mills IG, et al. Androgen receptor driven transcription in molecular apocrine breast cancer is mediated by FoxA1. EMBO J 2011;30:3019–27.
35. Iwafuchi-Doi M, Donahue G, Kakumanu A, Watts JA, Mahony S, Pugh BF, et al. The pioneer transcription Factor FoxA maintains an accessible nucleosome configuration at enhancers for tissue-specific gene activation. Mol Cell 2016;62:79–91.
36. Farmer P, Bonnefoi H, Becette V, Tubiana-Hulin M, Fumoleau P, Larsimont D, et al. Identification of molecular apocrine breast tumours by microarray analysis. Oncogene 2005;24:4660–71.
37. Doane AS, Danso M, Lal P, Donaton M, Zhang L, Hudis C, et al. An estrogen receptor-negative breast cancer subset characterized by a hormonally regulated transcriptional program and response to androgen. Oncogene 2006;25:3994–4008.
38. Lehmann BD, Bauer JA, Chen X, Sanders ME, Chakravarthy AB, Shyr Y, et al. Identification of human triple-negative breast cancer subtypes and preclinical models for selection of targeted therapies. J Clin Invest 2011; 121:2750–67.
39. Ni M, Chen Y, Lim E, Wimberly H, Bailey ST, Imai Y, et al. Targeting androgen receptor in estrogen receptor-negative breast cancer. Cancer Cell 2011;20:119–31.
40. Ni M, Chen Y, Fei T, Li D, Lim E, Liu XS, et al. Amplitude modulation of androgen signaling by c-MYC. Genes Dev 2013;27:734–48.
41. Attar N, Kurdistani SK. Exploitation of EP300 and CREBBP lysine acetyltransferases by cancer. Cold Spring Harb Perspect Med 2017;7:pii: a026534.
42. Zhong J, Ding L, Bohrer LR, Pan Y, Liu P, Zhang J, et al. P300 acetyltransferase regulates androgen receptor degradation and pten-deficient prostate tumorigenesis. Cancer Res 2014;74:1870–80.
43. Fu M, Wang C, Reutens AT, Wang J, Angeletti RH, Siconolfi-Baez L, et al. p300 and p300/cAMP-response element-binding protein-associated factor acetylate the androgen receptor at sites governing hormone-dependent transactivation. J Biol Chem 2000;275:20853–60.
44. Aarnisalo P, Palvimo JJ, Jänne OA. CREB-binding protein in androgen receptor-mediated signaling. Proc Natl Acad Sci U S A 1998;95:2122–7.
45. Cochrane DR, Bernales S, Jacobsen BM, Cittelly DM, Howe EN, D'Amato NC, et al. Role of the androgen receptor in breast cancer and preclinical analysis of enzalutamide. Breast Cancer Res 2014;16:R7.
46. Frønsdal K, Engedal N, Slagsvold T, Saatcioglu F. CREB binding protein is a coactivator for the androgen receptor and mediates cross-talk with AP-1. J Biol Chem 1998;273:31853–9.
47. Aarnisalo P, Palvimo JJ, Jänne OA. CREB-binding protein in androgen receptor-mediated signaling. Proc Natl Acad Sci U S A 1998;95:2122–7.
48. Ho Y, Dehm SM. Androgen receptor rearrangement and splicing variants in resistance to endocrine therapies in prostate cancer. Endocrinology 2017;158:1533–42.
49. Lasko LM, Jakob CG, Edalji RP, Qiu W, Montgomery D, Digiammarino EL, et al. Discovery of a selective catalytic p300/CBP inhibitor that targets lineage-specific tumours. Nature 2017;550:128–32.